

Deep Learning for Healthcare

Biomedicine Datalab

Master InterUniversitario de Data Science
Santander, Spain
March 2019

Ignacio Heredia
iheredia@ifca.unican.es
Instituto de Física de Cantabria
(CSIC-UC)

Table of contents

- Overview
- Images
 - Classification
 - Segmentation
 - Other tasks
- Time series
- Related fields
- Applications
 - The Good
 - The Bad
 - The Ugly



Coronavirus

Overview

Datasets

- [The MURA dataset](#): Musculoskeletal Radiographs
- [NIH Chest X-ray Dataset](#)
- [Qure25k](#): Head CT scans
- and [many more ...](#)

Groups

- [Deepmind Health](#)
- [Center for Artificial Intelligence in Medicine & Imaging](#)
- [MIT MediaLab](#)

Competitions on Kaggle

- [Médecine](#)
- [Healthcare](#)

Conferences & Workshops

- [ML4H: Machine Learning for Health](#) at NIPS
- [Towards Causal, Explainable and Universal Medical Visual Diagnosis](#) at CVPR
- [Medical Computer Vision](#) at CVPR
- [MICCAI](#)
- [Machine Learning for Healthcare](#)

Python modules

- [DeepChem](#) - DL for Drug Discovery

Overview - Reviews

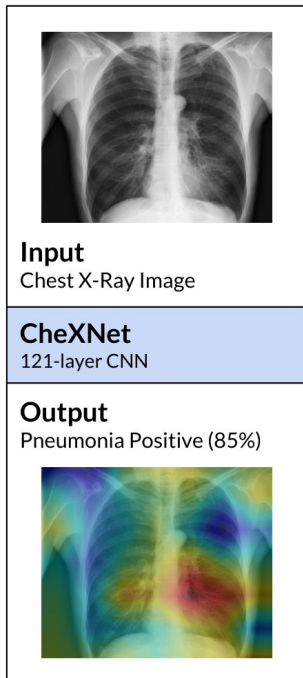
- Faust, O., Hagiwara, Y., Hong, T. J., Lih, O. S., & Acharya, U. R. (2018). [Deep learning for healthcare applications based on physiological signals: A review](#). Computer methods and programs in biomedicine, 161, 1-13.
- Miotto, R., Wang, F., Wang, S., Jiang, X., & Dudley, J. T. (2018). [Deep learning for healthcare: review, opportunities and challenges](#). Briefings in bioinformatics, 19(6), 1236-1246.
- Esteva, A., Robicquet, A., Ramsundar, B., Kuleshov, V., DePristo, M., Chou, K., ... & Dean, J. (2019). [A guide to deep learning in healthcare](#). Nature medicine, 25(1), 24-29.
- Beam, A. L., & Kohane, I. S. (2018). [Big data and machine learning in health care](#). Jama, 319(13), 1317-1318.
- Razzak, M. I., Naz, S., & Zaib, A. (2018). [Deep learning for medical image processing: Overview, challenges and the future](#). In Classification in BioApps (pp. 323-350). Springer, Cham.

Images

Image Classification

Pneumonia Detection on Chest X-Rays

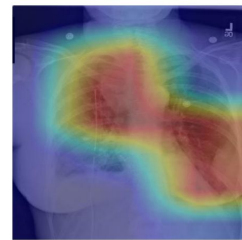
Rajpurkar, P., Irvin, J., Zhu, K., Yang, B., Mehta, H., Duan, T., ... & Lungren, M. P. (2017). [CheXNet: Radiologist-Level Pneumonia Detection on Chest X-Rays with Deep Learning](#). *arXiv preprint arXiv:1711.05225*.



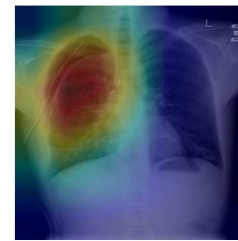
(a) Patient with multifocal community acquired pneumonia. The model correctly detects the airspace disease in the left lower and right upper lobes to arrive at the pneumonia diagnosis.



(b) Patient with a left lung nodule. The model identifies the left lower lobe lung nodule and correctly classifies the pathology.



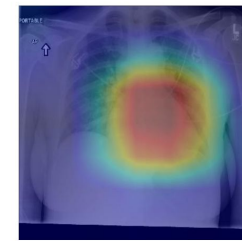
(c) Patient with primary lung malignancy and two large masses, one in the left lower lobe and one in the right upper lobe adjacent to the mediastinum. The model correctly identifies both masses in the X-ray.



(d) Patient with a right-sided pneumothorax and chest tube. The model detects the abnormal lung to correctly predict the presence of pneumothorax (collapsed lung).



(e) Patient with a large right pleural effusion (fluid in the pleural space). The model correctly labels the effusion and focuses on the right lower chest.

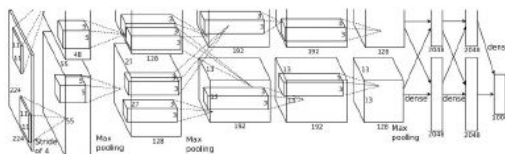
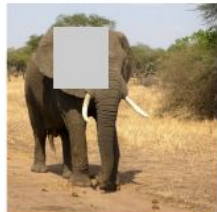


(f) Patient with congestive heart failure and cardiomegaly (enlarged heart). The model correctly identifies the enlarged cardiac silhouette.

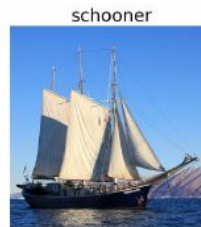
Reminder Saliency maps

Occlusion Experiments

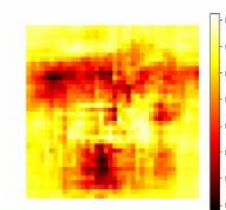
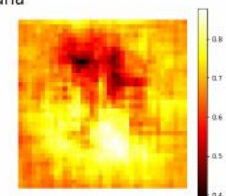
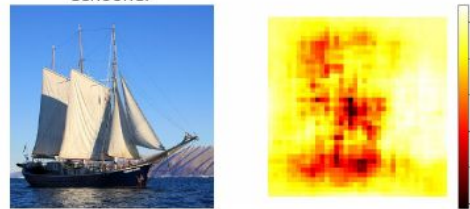
Mask part of the image before feeding to CNN, draw heatmap of probability at each mask location



Zeiler and Fergus, "Visualizing and Understanding Convolutional Networks", ECCV 2014



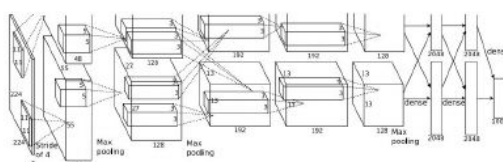
African elephant, Loxodonta africana



Reminder Saliency maps

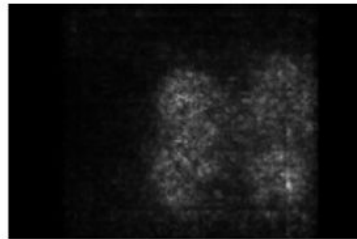
Saliency Maps

How to tell which pixels matter for classification?



Dog

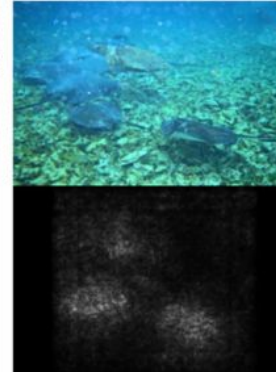
Compute gradient of (unnormalized) class score with respect to image pixels, take absolute value and max over RGB channels



Simonyan, Vedaldi, and Zisserman, "Deep Inside Convolutional Networks: Visualising Image Classification Models and Saliency Maps", ICLR Workshop 2014.
Figures copyright Karen Simonyan, Andrea Vedaldi, and Andrew Zisserman, 2014; reproduced with permission.

Reminder Saliency maps

Saliency Maps

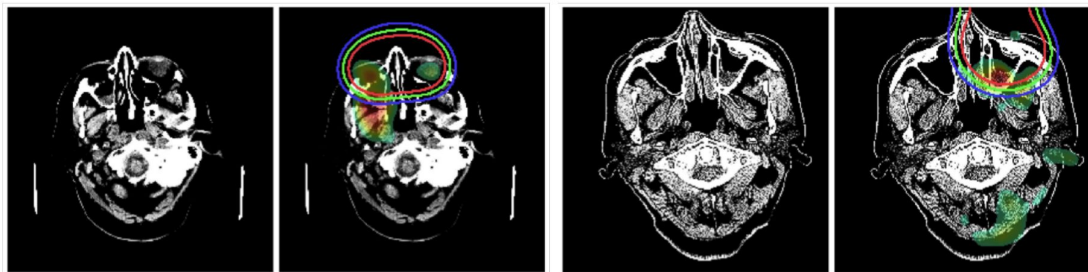


Simonyan, Vedaldi, and Zisserman, "Deep Inside Convolutional Networks: Visualising Image Classification Models and Saliency Maps", ICLR Workshop 2014.

Figures copyright Karen Simonyan, Andrea Vedaldi, and Andrew Zisserman, 2014; reproduced with permission.

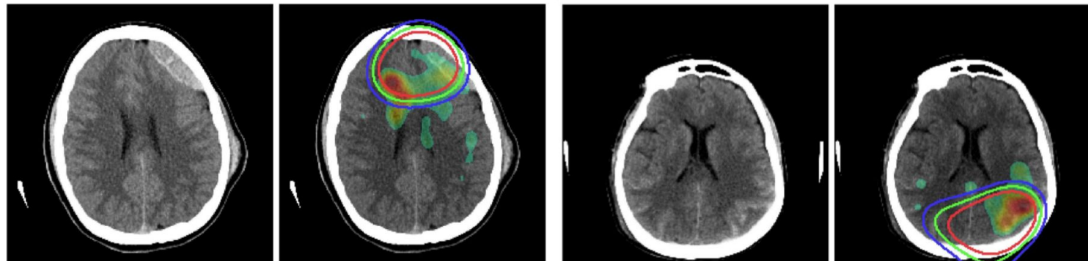
Pathology detection in CT images

Merkow, J., Luftkin, R., Nguyen, K., Soatto, S., Tu, Z., & Vedaldi, A. (2017). [DeepRadiologyNet: Radiologist Level Pathology Detection in CT Head Images](#). arXiv preprint arXiv:1711.09313.



(a)

(b)



(c)

(d)

Images

Image Segmentation

Reminder Image segmentation

- Label each pixel in the image with a category label.
- Don't differentiate instances, only care about pixels.

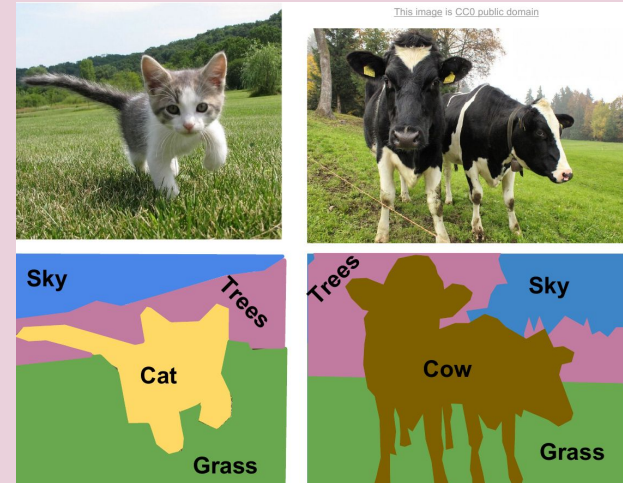
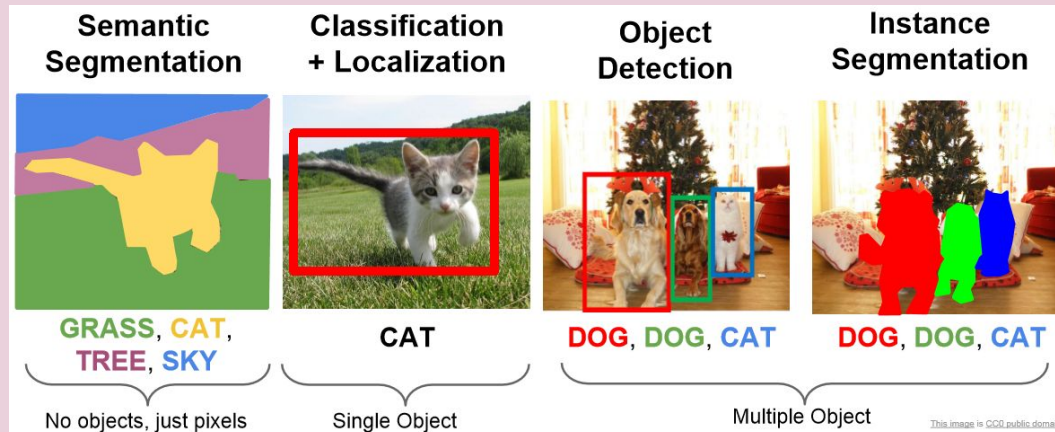
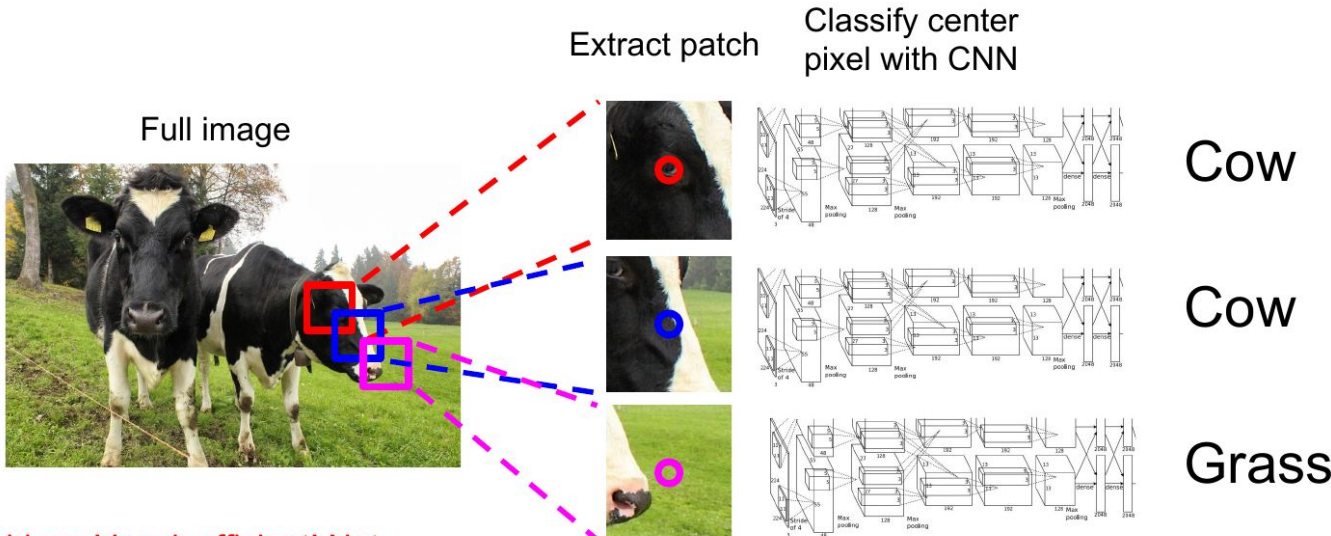


[Image source](#)

Reminder Image segmentation

Semantic Segmentation Idea: Sliding Window



Problem: Very inefficient! Not reusing shared features between overlapping patches

Farabet et al, "Learning Hierarchical Features for Scene Labeling," TPAMI 2013

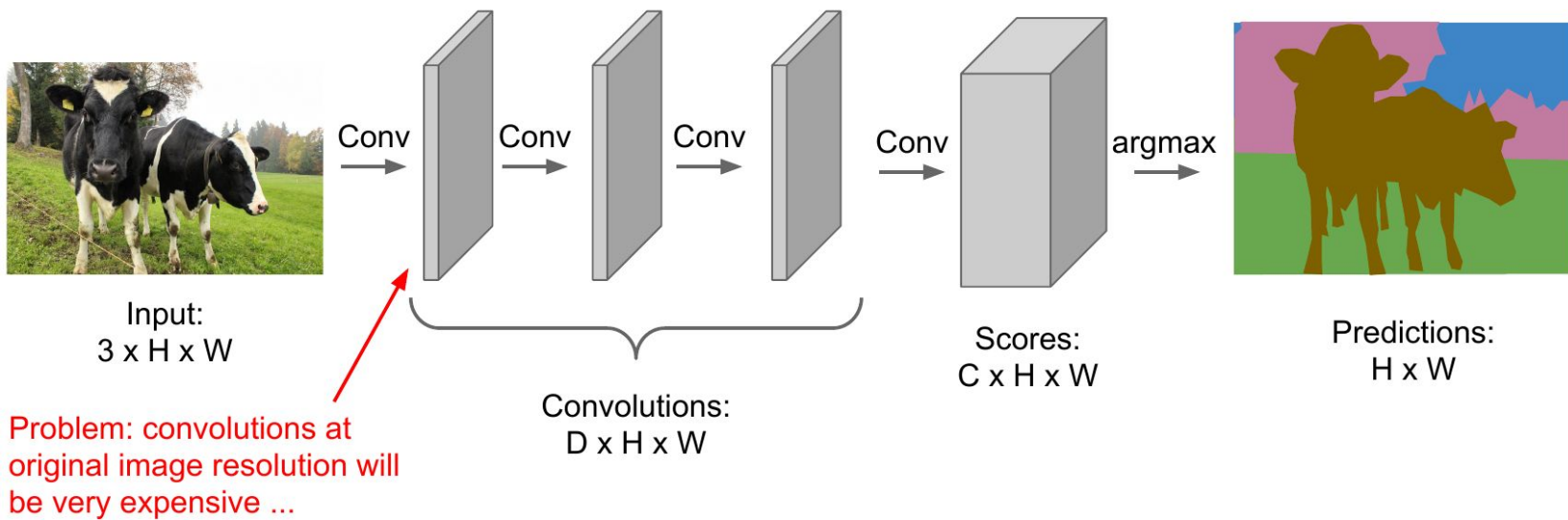
Pinheiro and Collobert, "Recurrent Convolutional Neural Networks for Scene Labeling", ICML 2014

[Image source](#)

Reminder Image segmentation

Semantic Segmentation Idea: Fully Convolutional

Design a network as a bunch of convolutional layers
to make predictions for pixels all at once!



Reminder Image segmentation

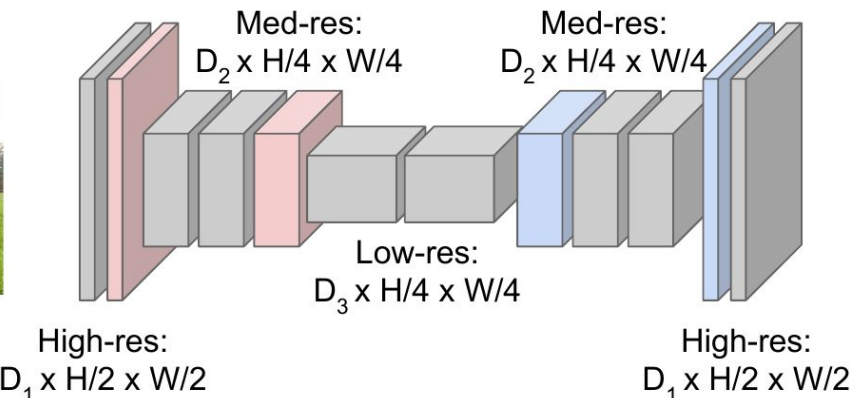
Semantic Segmentation Idea: Fully Convolutional

Downsampling:
Pooling, strided convolution



Input:
 $3 \times H \times W$

Design network as a bunch of convolutional layers, with
downsampling and **upsampling** inside the network!



Upsampling:
Unpooling or strided transpose convolution



Predictions:
 $H \times W$

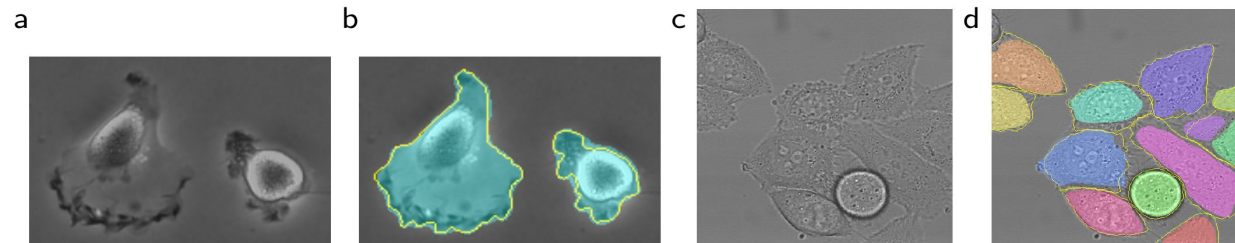
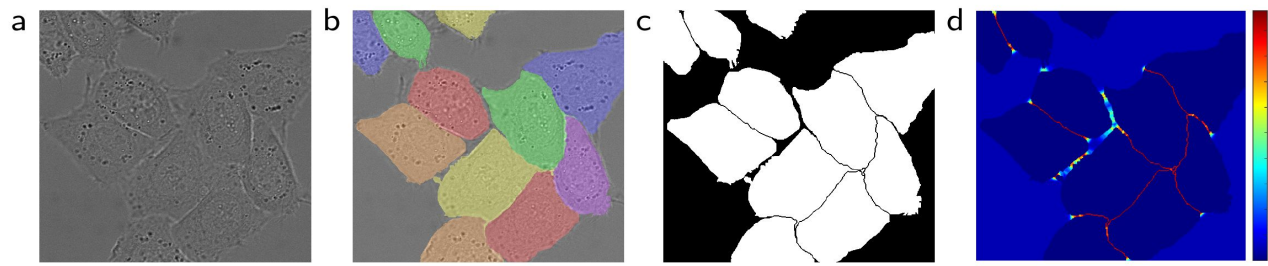
Long, Shelhamer, and Darrell, "Fully Convolutional Networks for Semantic Segmentation", CVPR 2015

Noh et al, "Learning Deconvolution Network for Semantic Segmentation", ICCV 2015

[Image source](#)

Biomedical image segmentation: U-Net

Ronneberger, O., Fischer, P., & Brox, T. (2015, October). [U-net: Convolutional networks for biomedical image segmentation](#). In *International Conference on Medical image computing and computer-assisted intervention* (pp. 234-241). Springer, Cham.



Brain tumor segmentation

Havaei, M., Davy, A., Warde-Farley, D., Biard, A., Courville, A., Bengio, Y., ... & Larochelle, H. (2017). [Brain tumor segmentation with deep neural networks](#). *Medical image analysis*, 35, 18-31.

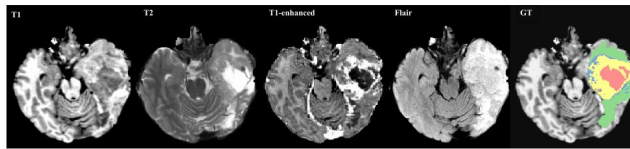


Figure 4: The first four images from left to right show the MRI modalities used as input channels to various CNN models and the fifth image shows the ground truth labels where ■ edema, ■ enhanced tumor, ■ necrosis, ■ non-enhanced tumor.

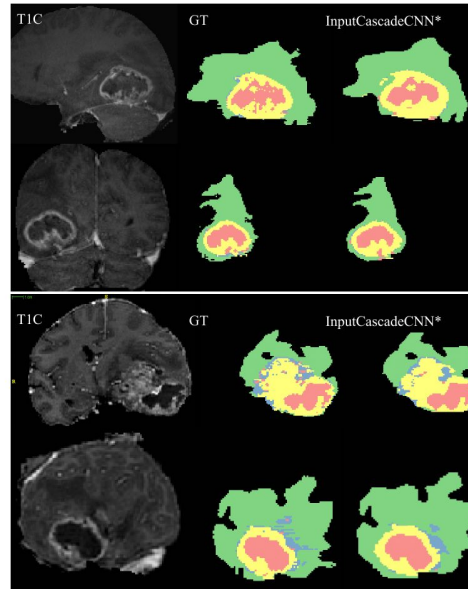
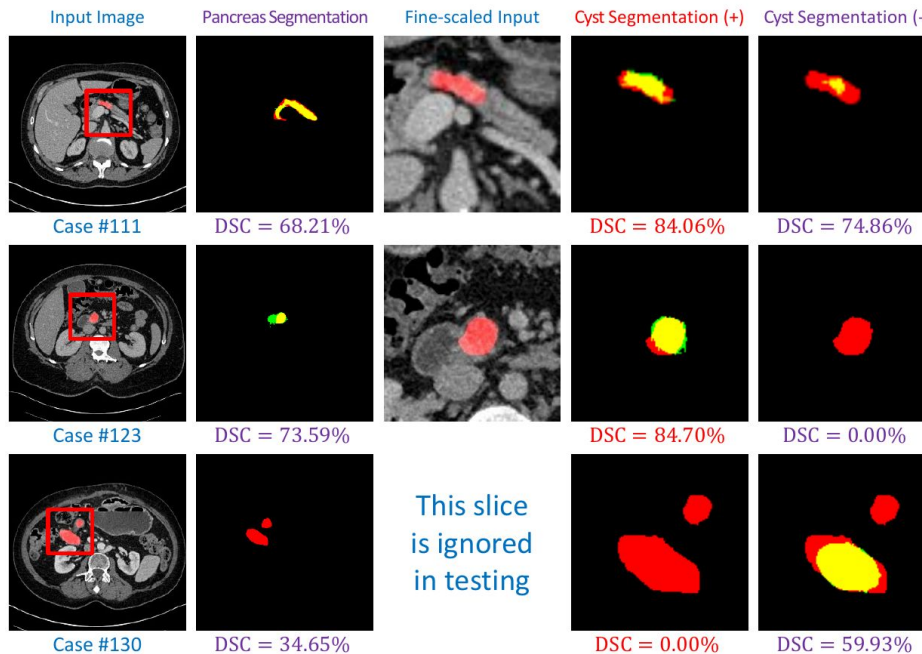


Figure 8: Visual results from our top performing model, INPUTCASCADECNN* on Coronal and Sagittal views. The subjects

Cyst segmentation

Zhou, Y., Xie, L., Fishman, E. K., & Yuille, A. L. (2017, September). [Deep supervision for pancreatic cyst segmentation in abdominal CT scans](#). In *International Conference on Medical Image Computing and Computer-Assisted Intervention* (pp. 222-230). Springer, Cham.



Skin cancer: detection and tracking

Li, Y., Esteva, A., Kuprel, B., Novoa, R., Ko, J., & Thrun, S. (2016). [Skin cancer detection and tracking using data synthesis and deep learning](#). *arXiv preprint arXiv:1612.01074*.

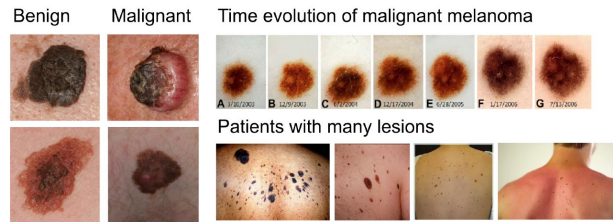


Figure 1: Key factors for skin cancer care include early detection and tracking over time.

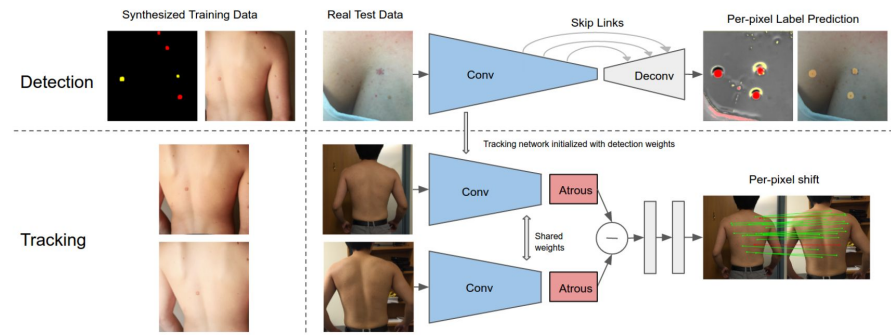


Figure 3: **Detection and Tracking System.** The network is trained on synthetic data and tested on real data. The detection network is composed of a conv section followed by a deconv section, with skip-link connections. In the top right we show the raw prediction heat map and the detection result after post processing. The tracking network takes the conv component of the detection network, and splits it up into a smaller conv part, and an atrous conv part. The two tracking images are each fed through the network and merged by a subtraction before the per-pixel shift prediction.

Segmenting without manual annotations

Zhang, L., Gopalakrishnan, V., Lu, L., Summers, R. M., Moss, J., & Yao, J. (2018). [Self-Learning to Detect and Segment Cysts in Lung CT Images without Manual Annotation](#). *arXiv preprint arXiv:1801.08486*.

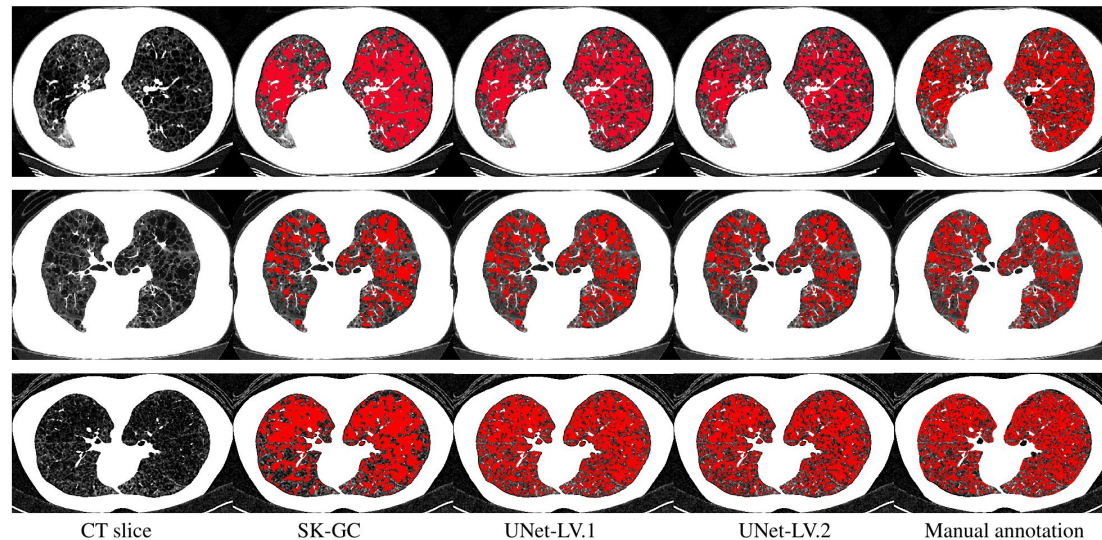


Fig. 3. Three examples (2 good image quality and 1 noisy) show segmentation results obtained by SK-GC, UNet-level1 and UNet-level2, given manual annotation as reference. UNet-level3 is not shown due to space constraint.

Fluorescence microscopy 3D segmentation

Fu, C., Lee, S., Ho, D. J., Han, S., Salama, P., Dunn, K. W., & Delp, E. J. (2018). [Fluorescence Microscopy Image Segmentation Using Convolutional Neural Network With Generative Adversarial Networks](#). *arXiv preprint arXiv:1801.07198*.

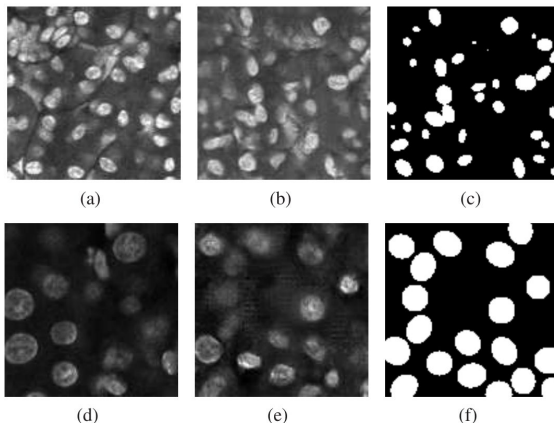


Fig. 3. Slices of the original volume and the corresponding synthetic volume for Data-I and Data-II (a) original image of Data-I, (b) synthetic image of Data-I, (c) synthetic binary image of Data-I (d) original image of Data-II, (e) synthetic image of Data-II, (f) synthetic binary image of Data-II.

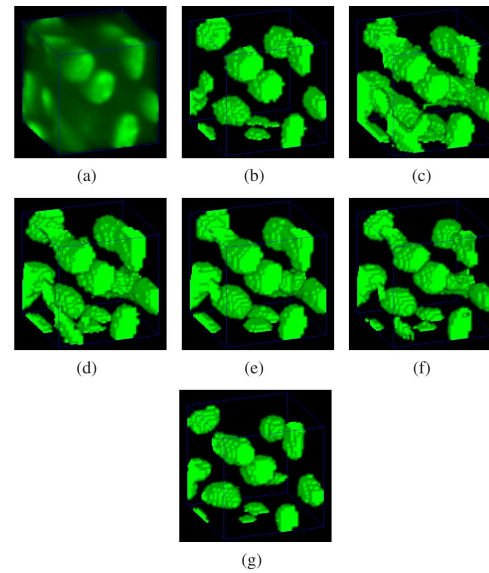


Fig. 4. 3D visualization of subvolume 1 of Data-I using Voxx [29] (a) original volume (b) 3D ground truth volume, (c) 3D active surfaces from [7], (d) 3D active surfaces with inhomogeneity correction from [8], (e) 3D Squash from [10][11], (f) 3D CNN from [22], (g) proposed method

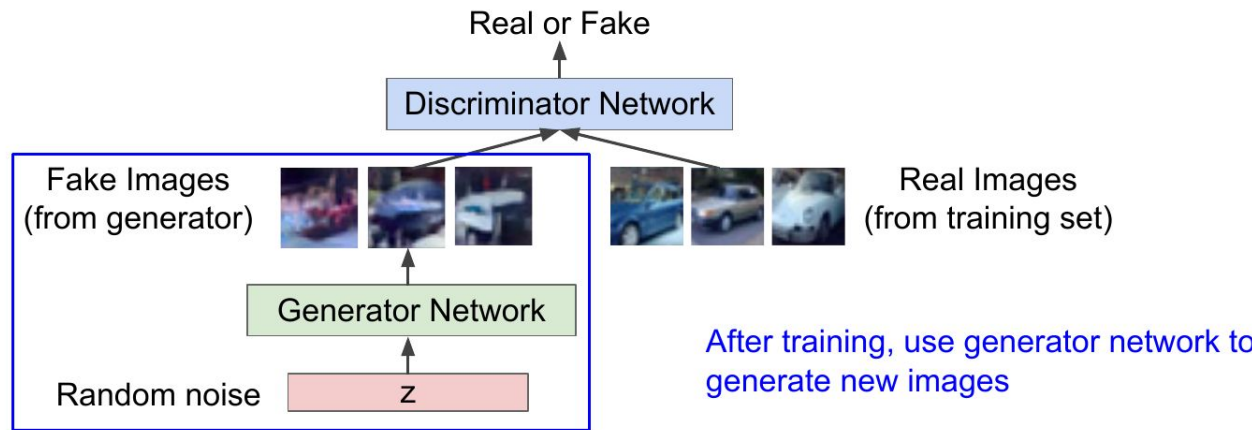
Reminder Generative Adversarial Networks

Training GANs: Two-player game

Ian Goodfellow et al., "Generative Adversarial Nets", NIPS 2014

Generator network: try to fool the discriminator by generating real-looking images

Discriminator network: try to distinguish between real and fake images



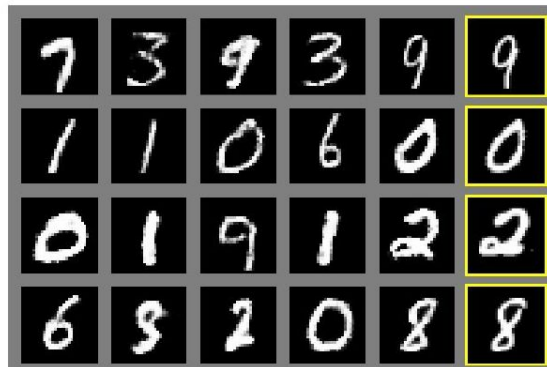
Fake and real images copyright Emily Denton et al. 2015. Reproduced with permission.

Reminder Generative Adversarial Networks

Ian Goodfellow et al., "Generative Adversarial Nets", NIPS 2014

Generative Adversarial Nets

Generated samples

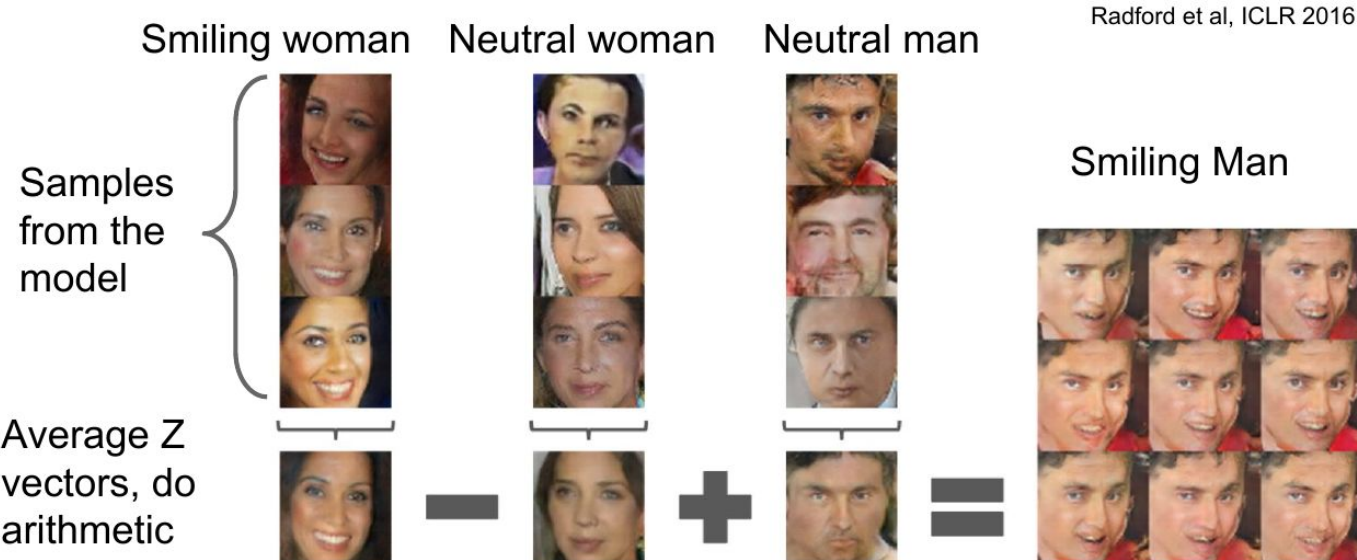


Nearest neighbor from training set

Figures copyright Ian Goodfellow et al., 2014. Reproduced with permission.

Reminder Generative Adversarial Networks

Generative Adversarial Nets: Interpretable Vector Math



Images

Other tasks

Automated image annotation

Shin, H. C., Roberts, K., Lu, L., Demner-Fushman, D., Yao, J., & Summers, R. M. (2016). [Learning to read chest x-rays: Recurrent neural cascade model for automated image annotation](#). In *Proceedings of the IEEE Conference on Computer Vision and Pattern Recognition* (pp. 2497-2506).

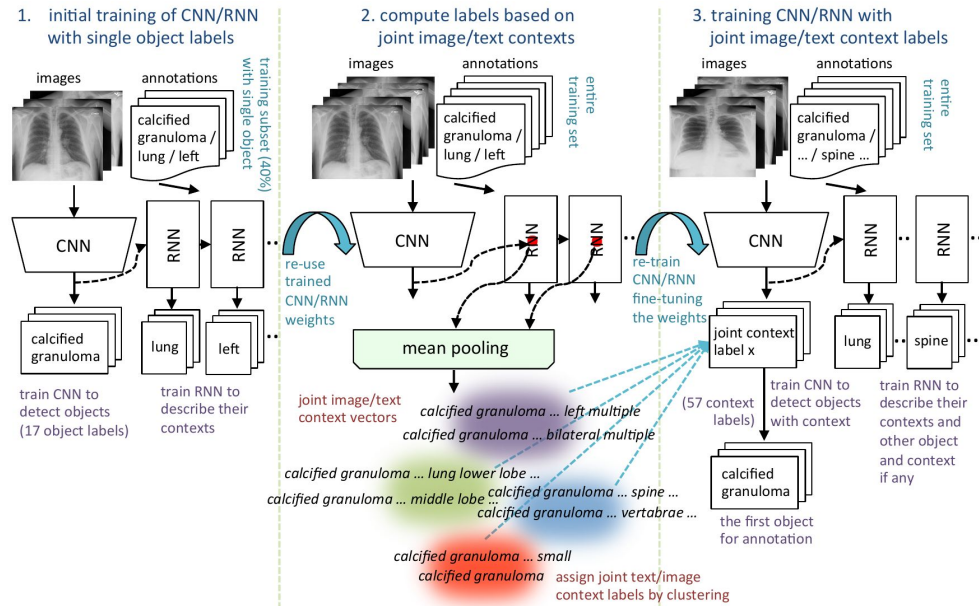


MeSH

Major
Pulmonary Atelectasis / lingula / focal
Calcinosis / lung / hilum / right

CHEST 2V FRONTAL/LATERAL XXXX, XXXX XXXX PM

Figure 1. An example of OpenI [2] chest x-ray image, report, and annotations.



Low dose PET image reconstruction

Xu, J., Gong, E., Pauly, J., & Zaharchuk, G. (2017). [200x Low-dose PET Reconstruction using Deep Learning](#). *arXiv preprint arXiv:1712.04119*.

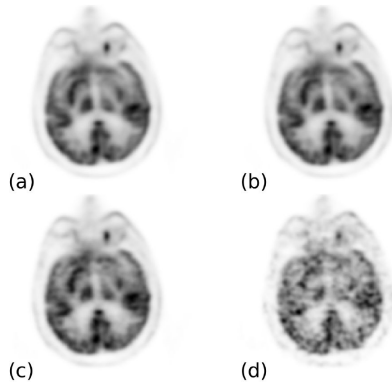


Fig. 1. PET images with normal dose and different levels of dose reduction. (a) standard-dose, (b) quarter-dose, (c) twentieth-dose, and (d) two-hundredth-dose.

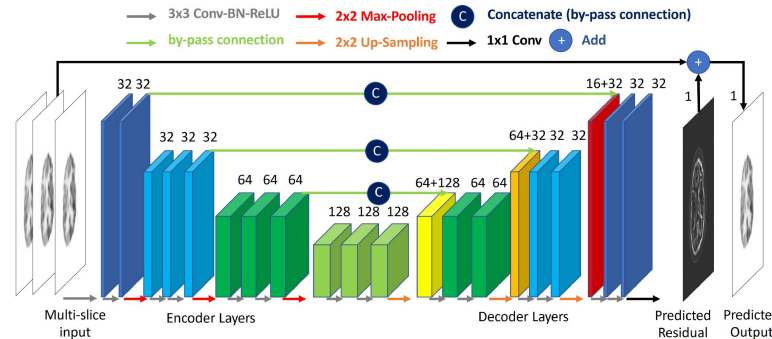


Fig. 2. Overall architecture of our proposed network.

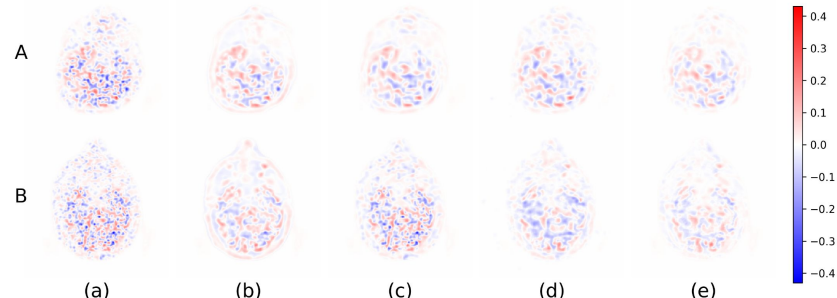


Fig. 8. Error map of Fig. 6 (a) low-dose, (b) NLM, (c)BM3D, (d) AC-Net, and (e) proposed.

Dental restoration

Hwang, Jyh-Jing, et al. "[Learning Beyond Human Expertise with Generative Models for Dental Restorations](#)." *arXiv preprint arXiv:1804.00064* (2018).

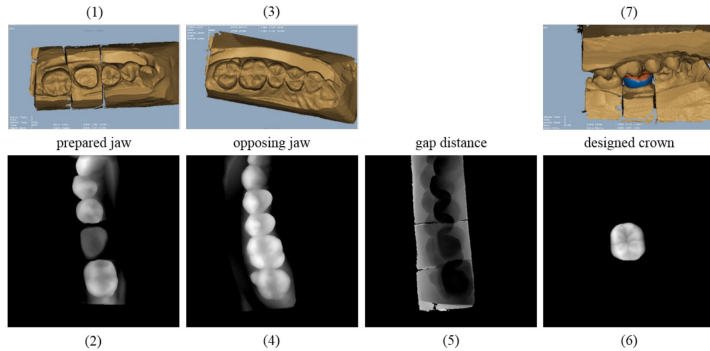


Fig. 1. Illustration of dental crown design stages. 3D models of the prepared jaw, opposing jaw, and the crown-filled restoration are shown at the top, and their 2D depth images from a particular plane shown below. The gap distances are computed from opposing jaws.

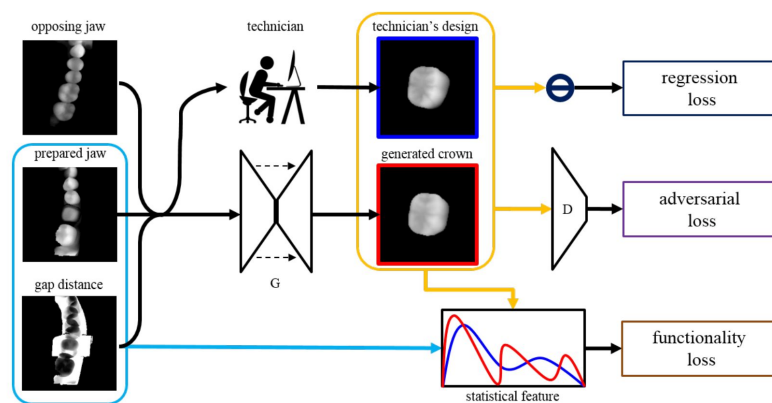


Fig. 2. Diagram illustration of the proposed model. We propose a functionality loss with space information (in the blue box) to learn the functionality of technician's designs. Please refer to Fig. 3 for the computation diagram of the functionality loss. (For all the crowns, we zoom in the images by a factor of 2 for better visualization.)

Diagnosing depression

Haque, Albert, et al. "[Measuring Depression Symptom Severity from Spoken Language and 3D Facial Expressions](#)." *arXiv preprint arXiv:1811.08592* (2018).

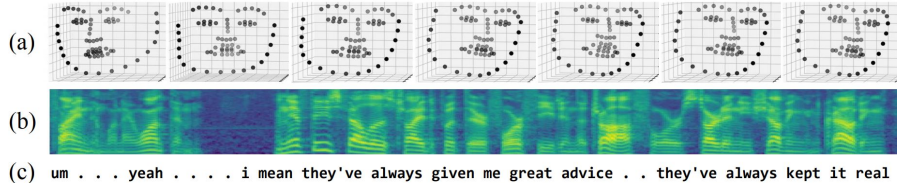


Figure 1: **Multi-modal data.** For each clinical interview, we use: (a) video of 3D facial scans, (b) audio recording, visualized as a log-mel spectrogram, and (c) text transcription of the patient's speech. Our model predicts the severity of depressive symptoms using all three modalities.

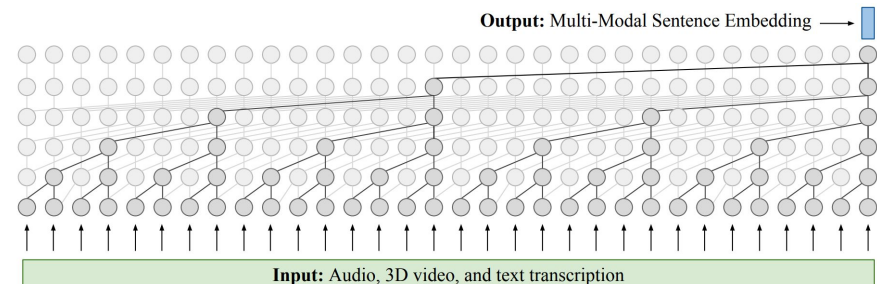
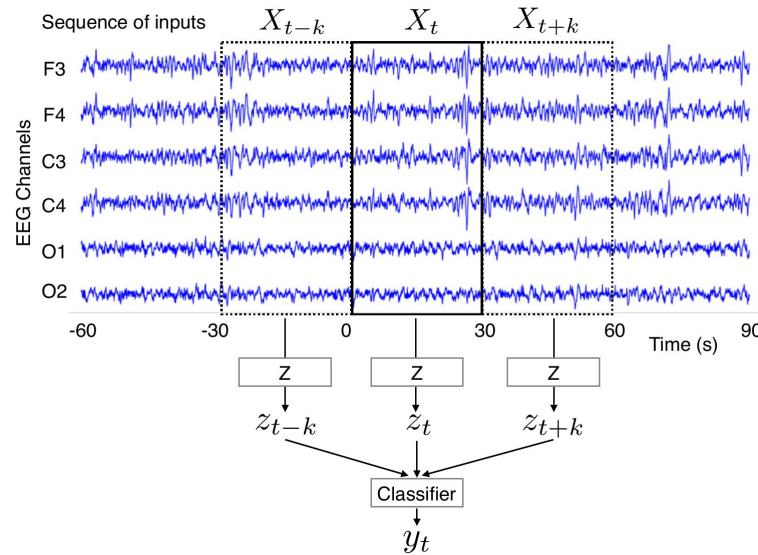


Figure 2: **Our method: Learning a multi-modal sentence embedding.** Overall, our model is a causal CNN [5]. The input to our model is: audio, 3D facial scans, and text. The multi-modal sentence embedding is fed to a depression classifier and PHQ regression model (not shown above).

Time series

Classifying sleep stages

Chambon, S., Galtier, M., Arnal, P., Wainrib, G., & Gramfort, A. (2017). [A deep learning architecture for temporal sleep stage classification using multivariate and multimodal time series](#). arXiv preprint arXiv:1707.03321.



Detecting arrhythmia

Rajpurkar, P., Hannun, A. Y., Haghpanahi, M., Bourn, C., & Ng, A. Y. (2017). [Cardiologist-level arrhythmia detection with convolutional neural networks](#). *arXiv preprint arXiv:1707.01836*.

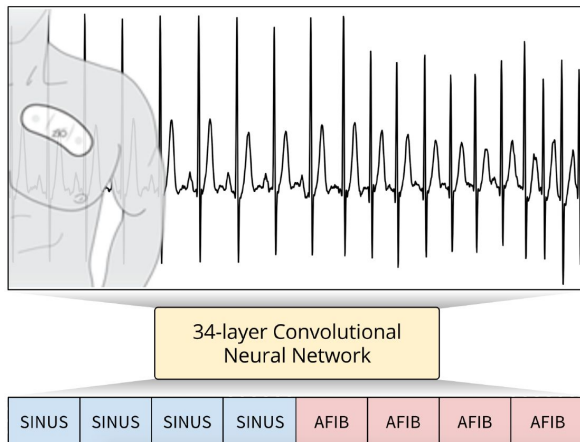


Figure 1. Our trained convolutional neural network correctly detecting the sinus rhythm (SINUS) and Atrial Fibrillation (AFIB) from this ECG recorded with a single-lead wearable heart monitor.

	Seq		Set	
	Model	Cardiol.	Model	Cardiol.
Class-level F1 Score				
AFIB	0.604	0.515	0.667	0.544
AFL	0.687	0.635	0.679	0.646
AVB_TYPE2	0.689	0.535	0.656	0.529
BIGEMINY	0.897	0.837	0.870	0.849
CHB	0.843	0.701	0.852	0.685
EAR	0.519	0.476	0.571	0.529
IVR	0.761	0.632	0.774	0.720
JUNCTIONAL	0.670	0.684	0.783	0.674
NOISE	0.823	0.768	0.704	0.689
SINUS	0.879	0.847	0.939	0.907
SVT	0.477	0.449	0.658	0.556
TRIGEMINY	0.908	0.843	0.870	0.816
VT	0.506	0.566	0.694	0.769
WENCKEBACH	0.709	0.593	0.806	0.736
Aggregate Results				
Precision (PPV)	0.800	0.723	0.809	0.763
Recall (Sensitivity)	0.784	0.724	0.827	0.744
F1	0.776	0.719	0.809	0.751

Table 1. The top part of the table gives a class-level comparison of the expert to the model F1 score for both the Sequence and the Set metrics. The bottom part of the table shows aggregate results over the full test set for precision, recall and F1 for both the Sequence and Set metrics.

Predicting blood pressure

Su, P., Ding, X., Zhang, Y., Li, Y., & Zhao, N. (2017). [Predicting Blood Pressure with Deep Bidirectional LSTM Network](#). *arXiv preprint arXiv:1705.04524*.

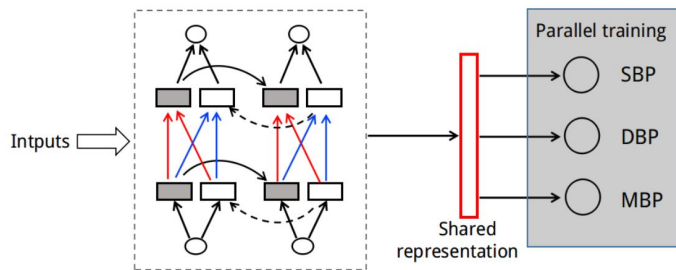


Figure 4: Multitask training pipeline. Training the model to predict SBP, DBP and MBP in parallel while using a shared data representation learned by lower hidden layers. And what is learned for each task can help other tasks to be learned better.

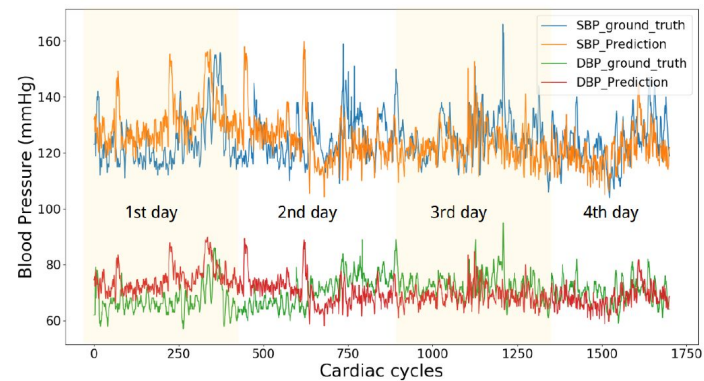
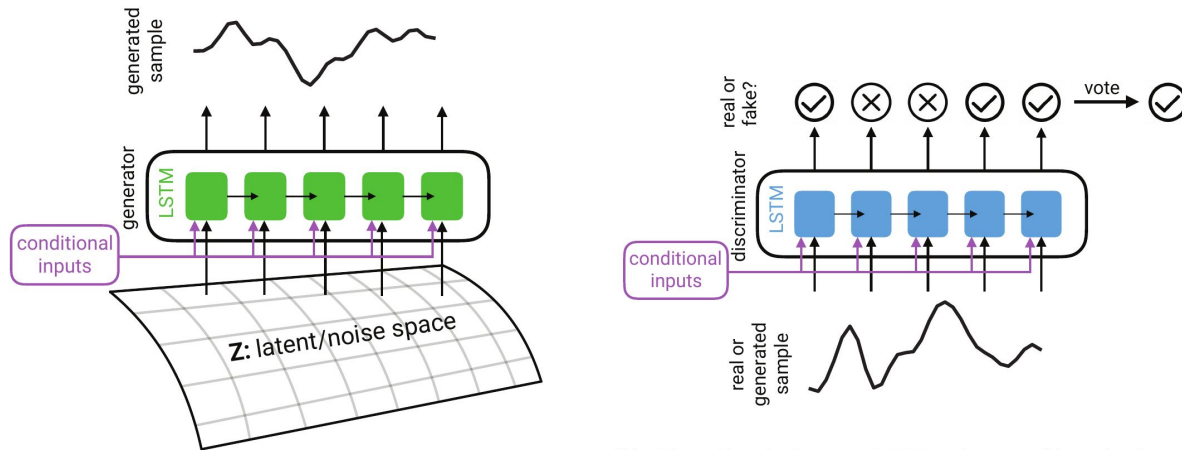


Figure 5: Comparison of the ground truth and DM-LSTM model prediction on a four-day BP sequence of one representative subject. The result suggests that our DM-LSTM model can effectively learn the multi-timescale dependencies.

Generating realistic time series

Esteban, C., Hyland, S. L., & Rätsch, G. (2017). [Real-valued \(medical\) time series generation with recurrent conditional GANs](#). *arXiv preprint arXiv:1706.02633*.



(a) The generator RNN takes a different random seed at each temporal input, and produces a synthetic signal. In the case of the RCGAN, it also takes an additional input on each time step that conditions the output.

(b) The discriminator RNN takes real/synthetic sequences and produces a classification into real/synthetic for each time step. In the case of the RCGAN, it also takes an additional input on each time step that conditions the output.

Figure 1: Architecture of Recurrent GAN and Conditional Recurrent GAN models.

Predicting pregnancy probabilities

Liu, Bo, et al. "Predicting pregnancy using large-scale data from a women's health tracking mobile application." *arXiv preprint arXiv:1812.02222* (2018).

Table 1: All daily features which appear in our data. Each feature has both a category and a type. Features are binary except for those in the “continuous” category. While pregnancy tests are included in the binary features, we do not use them as predictive features. HBC=hormonal birth control; TNP=type not provided.

Category	Type
Ailment	Allergy, Cold/Flu Ailment, Fever, Injury
Appointment	Date, Doctor, Ob Gyn, Vacation
Collection Method	Menstrual Cup, Pad, Panty Liner, Tampon
Continuous	BBT, Resting Heart Rate, Weight
Craving	Carbs, Chocolate, Salty, Sweet
Digestion	Bloated, Gassy, Great Digestion, Nauseated
Emotion	Happy, PMS, Sad, Sensitive
Energy	Energized, Exhausted, High Energy, Low Energy
Exercise	Biking, Running, Swimming, Yoga
Fluid	Atypical, Creamy, Egg White, Sticky
Hair	Bad, Dry, Good, Oily
Injection HBC	Administered, Type Not Provided
IUD	Inserted, Removed, Thread Checked, TNP
Medication	Antibiotic, Antihistamine, Cold/Flu Medication, Pain
Mental	Calm, Distracted, Focused, Stressed
Motivation	Motivated, Productive, Unmotivated, Unproductive
Pain	Cramps, Headache, Ovulation Pain, Tender Breasts
Party	Big Night Party, Cigarettes, Drinks Party, Hangover
Patch HBC	Removed, Removed Late, Replaced, Replaced Late, TNP
Period	Heavy, Light, Medium, Spotting
Pill HBC	Double, Late, Missed, Taken, TNP
Poop	Constipated, Diarrhea, Great, Normal
Ring HBC	Removed, Removed Late, Replaced, Replaced Late, TNP
Sex	High Sex Drive, Protected, Unprotected, Withdrawal
Skin	Acne, Dry, Good, Oily
Sleep	0-3 Hrs, 3-6 Hrs, 6-9 Hrs, 9 Hrs, TNP
Social	Conflict, Sociable, Supportive, Withdrawn
Test	Ovulation Neg, Ovulation Pos, Pregnancy Neg, Pregnancy Pos

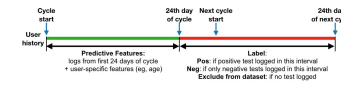


Figure 1: Prediction task. The model makes predictions using logs from the first 24 days of a cycle (green interval), and the cycle is labeled using pregnancy tests taken after day 24 of the cycle and before day 24 of the next cycle (red interval). The vast majority of pregnancy tests in our dataset are taken near when the user's cycle is supposed to start, consistent with proper use of pregnancy tests, so any positive pregnancy tests likely result from activity during the green interval, which will be included in the feature vector.

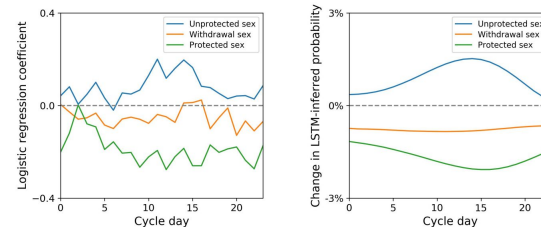


Figure 4: Model-learned time trends are interpretable for both the simple logistic regression model (left plot) and the best-performing LSTM + user embedding model (right plot). The horizontal axis is the cycle day. The vertical axis in the left plot is the logistic regression weight for logging a feature on that cycle day. The vertical axis in the right plot is how much logging a feature on a cycle day affects the LSTM-inferred probability of pregnancy. In both plots, positive y-values indicate associations with positive pregnancy tests, and negative y-values indicate associations with negative pregnancy tests. Both models learn that protected sex (green line) is negatively associated with pregnancy, while unprotected sex (blue line) is positively associated, particularly during the fertile window, and withdrawal sex (orange line) is intermediate.

Machine translation of cortical activity

Makin, J. G., Moses, D. A., & Chang, E. F. (2020). [Machine translation of cortical activity to text with an encoder-decoder framework](#) (pp. 1-8). Nature Publishing Group.

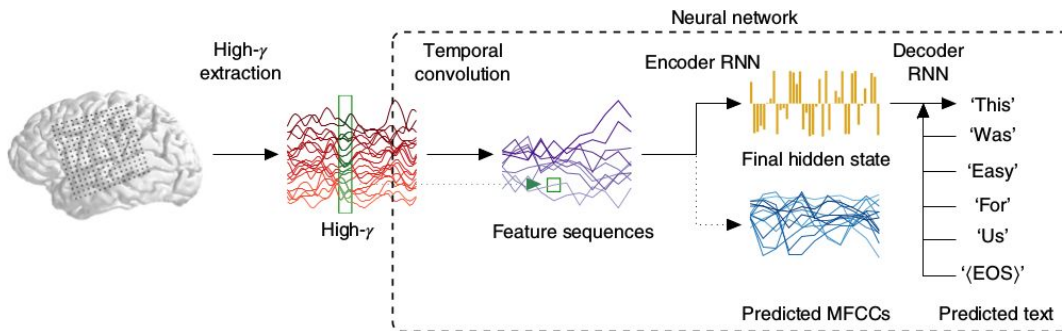


Fig. 1 | The decoding pipeline. Each participant read sentences from one of two datasets (MOCHA-TIMIT, picture descriptions) while neural signals were recorded with an ECoG array (120–250 electrodes) covering peri-Sylvian cortices. The analytic amplitudes of the high- γ signals (70–150 Hz) were extracted at about 200 Hz, clipped to the length of the spoken sentences and supplied as input to an artificial neural network. The early stages of the network learn temporal convolutional filters that, additionally, effectively downsample these signals. Each filter maps data from 12-sample-wide windows across all electrodes (for example, the green window shown on the example high- γ signals in red) to single samples of a feature sequence (highlighted in the green square on the blue feature sequences); then slides by 12 input samples to produce the next sample of the feature sequence; and so on. One hundred feature sequences are produced in this way, and then passed to the encoder RNN, which learns to summarize them in a single hidden state. The encoder RNN is also trained to predict the MFCCs of the speech audio signal that temporally coincide with the ECoG data, although these are not used during testing (see “The decoder pipeline” for details). The final encoder hidden state initializes the decoder RNN, which learns to predict the next word in the sequence, given the previous word and its own current state. During testing, the previous predicted word is used instead.

Treatments based on Reinforcement Learning

Raghu, Aniruddh, Matthieu Komorowski, and Sumeetpal Singh. "[Model-Based Reinforcement Learning for Sepsis Treatment](#)." *arXiv preprint arXiv:1811.09602* (2018).

Related fields

Health related fields

Deep learning is being used in a lot of adjacent fields that could benefit healthcare:

- Genomics
 - gene expression: characterization and prediction
 - regulatory genomics: promoters and enhancers, splicing, transcription factors and RNA binding proteins
 - functional genomics: mutations and functional activities, subcellular localization
 - structural genomics: classification of proteins, protein secondary structure, protein tertiary structure and quality assessment, contact map
- Computational chemistry
 - computer-aided drug design
 - computational structural biology
 - quantum chemistry
 - computational material design

Health related fields - Protein structure prediction

Senior, A. W., Evans, R., Jumper, J., Kirkpatrick, J., Sifre, L., Green, T., ... & Penedones, H. (2020). [Improved protein structure prediction using potentials from deep learning](#). *Nature*, 1-5.

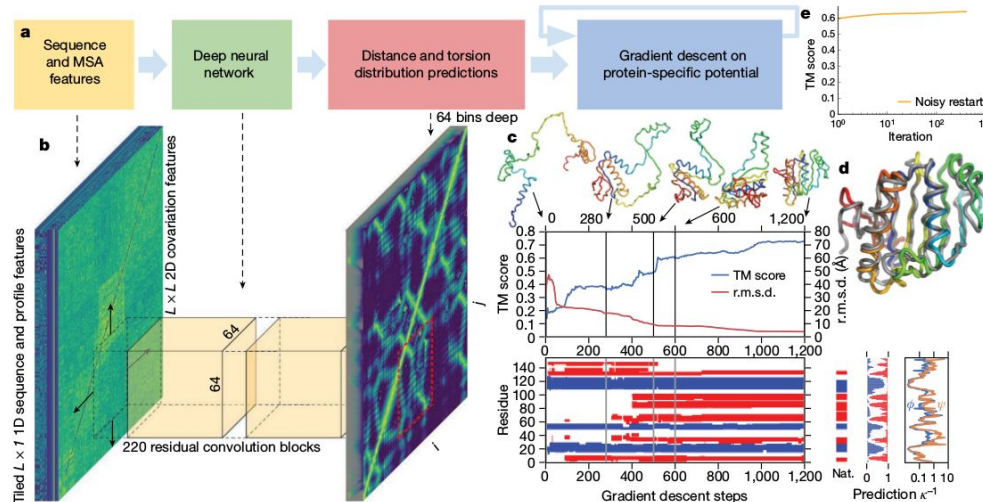


Fig. 2 | The folding process illustrated for CASP13 target T0986s2. CASP target T0986s2, $L = 155$, PDB: 6N9V. **a**, Steps of structure prediction. **b**, The neural network predicts the entire $L \times L$ histogram based on MSA features, accumulating separate predictions for 64×64 -residue regions. **c**, One iteration of gradient descent (1,200 steps) is shown, with the TM score and root mean square deviation (r.m.s.d.) plotted against step number with five snapshots of the structure. The secondary structure (from SST³³) is also shown (helix in blue, strand in red) along with the native secondary structure (Nat.). The secondary

structure prediction probabilities of the network and the uncertainty in torsion angle predictions (as κ^{-1} of the von Mises distributions fitted to the predictions for ϕ and ψ). While each step of gradient descent greedily lowers the potential, large global conformation changes are effected, resulting in a well-packed chain. **d**, The final first submission overlaid on the native structure (in grey). **e**, The average (across the test set, $n=377$) TM score of the lowest-potential structure against the number of repeats of gradient descent per target (log scale).

Real world applications

Applications - The Good

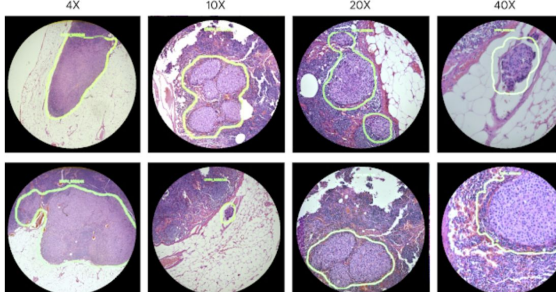
- Lots of potentially beneficial real world applications

Google made an AR microscope that can help detect cancer

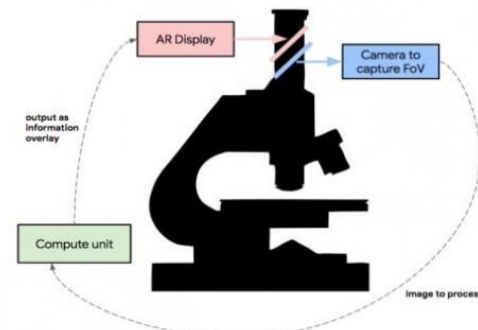
AI algorithms detect and highlight cancer cells in images of human tissue.

Mallory Locklear, @mallorylocklear
04.16.18 in Medicine

0 Comments | 3005 Shares

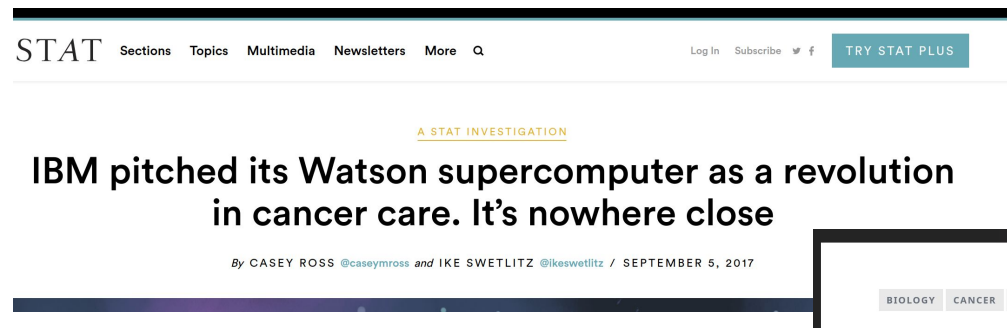


The image shows a screenshot of a social media post from Mallory Locklear (@mallorylocklear) dated April 16, 2018, in the 'Medicine' category. The post features a grid of eight microscopy images of tissue samples at various magnifications (4X, 10X, 20X, 40X). AI algorithms have highlighted specific areas of interest with yellow outlines in several of the images.



Applications - The Bad

- Some real world applications fail to meet expectations



The screenshot shows a news article from STAT titled "IBM pitched its Watson supercomputer as a revolution in cancer care. It's nowhere close". The article is dated September 5, 2017, and is attributed to CASEY ROSS and IKE SWETLITZ. The main headline features a photo of a game show set with a large screen displaying "\$200,000" and a question about Bram Stoker. Below the headline, a sub-headline reads "IBM's Watson versus cancer: Hype meets reality". A brief summary at the bottom states that five years ago, IBM announced Watson would revolutionize cancer treatment, but a recent report shows it hasn't lived up to expectations.

STAT Sections Topics Multimedia Newsletters More Q Log In Subscribe [Twitter](#) [Facebook](#) TRY STAT PLUS

A STAT INVESTIGATION

IBM pitched its Watson supercomputer as a revolution in cancer care. It's nowhere close

By CASEY ROSS @caseymross and IKE SWETLITZ @ikeswetlitz / SEPTEMBER 5, 2017

IBM's Watson versus cancer: Hype meets reality

Five years ago, IBM announced that its supercomputer Watson would revolutionize cancer treatment by using its artificial intelligence to digest and distill the thousands of oncology studies published every year plus patient-level data and expert recommendations into treatment recommendation. Last week, a report published by STAT News shows that, years later, IBM's hubris and hype have crashed into reality.

Who is Bram Stoker?

\$200,000

\$300,000

\$100,000

\$17,973

\$5600

David Gorski on September 11, 2017



The screenshot shows a blog post titled "IBM Watson: Not living up to hype as a tool to fight cancer?". The post is by Orac and was published on September 18, 2017. It has 31 comments. The post discusses the same topic as the STAT article, pointing out that while IBM claimed Watson would revolutionize cancer treatment, it has not delivered on that promise.

BIOLOGY CANCER COMPUTERS

IBM Watson: Not living up to hype as a tool to fight cancer?

Orac | September 18, 2017 | 31 Comments

Applications - The Ugly

- Privacy concerns



WIRED

WIRED Security

AI has no place in the NHS if patient privacy isn't assured

DeepMind is working on a technical solution to boost transparency when it comes to AI in healthcare – but it's a long road to machines gaining patient trust

Google DeepMind 1.6m patient record deal 'inappropriate'

National data guardian says patient data transfer from Royal Free to Google subsidiary has 'inappropriate legal basis' as information not used for direct care

Applications - Coronavirus



Review: Bullock, J., Pham, K. H., Lam, C. S. N., & Luengo-Oroz, M. (2020). [Mapping the Landscape of Artificial Intelligence Applications against COVID-19](#). arXiv preprint arXiv:2003.11336.

Examples:

- Wang, L., & Wong, A. (2020). [COVID-Net: A tailored deep convolutional neural network design for detection of COVID-19 cases from chest radiography images](#). arXiv preprint arXiv:2003.09871.
- John Jumper, Kathryn Tunyasuvunakool, Pushmeet Kohli, Demis Hassabis, and the AlphaFold Team, "[Computational predictions of protein structures associated with COVID-19](#)", Version 2, DeepMind website, 8 April 2020
- Pal, R., Sekh, A. A., Kar, S., & Prasad, D. K. (2020). [Neural network based country wise risk prediction of COVID-19](#). arXiv preprint arXiv:2004.00959.
- Hofmarcher, M., Mayr, A., Rumetshofer, E., Ruch, P., Renz, P., Schimunek, J., ... & Klambauer, G. (2020). [Large-scale ligand-based virtual screening for SARS-CoV-2 inhibitors using deep neural networks](#). Available at SSRN 3561442.
- ...

Questions